THE TRUE BEHAVIOR OF THIN CONCRETE BRIDGE SLABS

P. Csagoly, M. Holowka and R. Dorton, Ontario Ministry of Transportation and Communications

It has been observed that thin concrete deck slabs supported by beams or girders are generally capable of carrying concentrated wheel loads far in excess of design values established by traditional methods of analysis. This capacity appears to be present even if the concrete has considerably deteriorated or a large percentage of the reinforcing steel is lost due to rusting. The usual failure mode is that of punching and not flexure, hence the load-carrying capacity is defined in terms of the former. Under a concentrated wheel load, the present AASHTO Specifications, based on 2-dimensional plate bending theory, overestimate the maximum tensile reinforcing steel stresses by a considerable margin. It has been found that the load-carrying capacity of the slab is governed by internal arching action, rather than by flexural strength. The net result is that a multiple of the absolute minimum reinforcing is being built into thin concrete deck slabs. In the presence of deicing salt, too much steel too close to the wearing surface usually results in extensive spalling of the concrete decks, leading to a marked reduction in service life. This paper covers the results of an extensive prototype investigation. Field testing of existing bridges, both composite and non-composite, deteriorated and not deteriorated, with a 445 kN (1000,000 lb.) simulated wheel load resulted in no permanent damage or upper surface cracking to the slabs. New prototype deck slabs have been built with as little as 0.2% isotropic reinforcement. The test results indicate sufficient capacity for concentrated wheel loads with steel stresses and deflection being at acceptable levels. These research findings are being incorporated into the new Ontario Highway Bridge Design Code.

In the Province of Ontario, as in most North American jurisdictions, the design of thin concrete bridge decks supported by girders and/or beams is based at present on the AASHTO Specifications for Highway Bridges (1). The deck may be designed to act only as the riding surface or, alternatively, it may be considered composite with the supporting components if shear connectors are employed. The beams or girders may be of concrete, prestressed concrete, timber or steel. The geometry of supporting components can be of various types: rectangular, with or without voids, I-shaped, and open or closed box sections.

The fundamental concept behind the AASHTO provisions is that these slabs, subdivided into transverse strips for design convenience, are carrying concentrated wheel loads entirely in flexure. The format of calculations, until 1974, was based on the working stress method. This approach, without altering the fundamental concept, has been recently modified and a load factor method is now used (2). It is also assumed that slabs designed for bending moment in accordance with the AASHTO Specifications can be considered safe regarding bond and shear.

The authors maintain that these concrete slabs are greatly over-designed and that a new design approach should be developed. This type of bridge superstructure is the most common design in Ontario (and also in the United States) and significant savings in construction costs could be anticipated by an improved design method. On the basis of this anticipation, a series of projects sponsored by the Ontario Ministry of Transportation and Communications' Joint Highway Research Program was initiated at Queen's University in Kingston, Ontario, in 1967. The ultimate aim of these projects was to investigate the load-carrying capacity of composite I-beam bridges.

Another recent problem with concrete decks is spalling (3) resulting from reinforcement corrosion due to deicing salts. Corrosion, among other factors, is directly related to the depth of cover over the reinforcement. A more meaningful parameter is the ratio of clear cover to bar diameter (C/D). It is believed that a C/D value of 3.0 can provide reasonably good protection. Reducing the reinforcing steel requirements can mean smaller bar sizes and, consequently, increased concrete cover-to-diameter ratio — thereby improving the durability of exposed concrete bridge decks. A better understanding of their behavior may also lead to increasing the absolute cover without substantially reducing the load-carrying capacity of these slabs.

This paper describes part of the research work conducted by the Ministry to verify and to

implement a revolutionary new method of slab design based on the theoretical model for ultimate load capacity of the slab as developed at Queen's University (4, 5). The physical work included field testing of existing concrete decks and the design and testing of prototype full-scale decks built in accordance with the new theoretical model. In this paper, only the field testing of old, existing bridges is discussed in detail. The effects of using reduced amounts of reinforcement in prototype bridges are reported elsewhere (6, 7). The results confirm the existence of large ultimate capacities of the slabs as predicted by the theoretical model.

Recommendations are given to simplify the design of most concrete decks, to substantially reduce the reinforcing steel requirement and to develop standardization of deck reinforcement.

Background

The initial research conducted at Queen's University indicated that the ultimate strength of concrete deck slabs of composite steel/concrete bridges under concentrated load was about one order higher than predicted by the AASHTO design method. It was also observed that the mode of failure is in punching shear, not flexure, suggesting the presence of considerable membrane forces providing for load-carrying by internal arching.

It was also shown that satisfactory factors of safety against failure by punching can be anticipated even with reduced slab reinforcement as illustrated in Figure 1. It can be seen that the effect of reducing the amount of reinforcement from the customary 1.0 to 0.2% causes a drop of about 20% in the load-carrying capacity at the practical span-to-thickness ratio. It is also evident, that the most important parameter is this ratio. In Appendix A it is shown that stresses, regardless whether related to flexure or internal arching, decrease with the square of the slab thickness.

The ultimate capacity is greatly influenced by the degree of lateral restraints present (Figure 2). These restraints prevent the horizontal movement and rotation of the slab adjacent to the point load by developing forces due to the physical boundary conditions such as massive continuity of slab, bracings, diaphragms, shear connectors and laterally stiff beams. However, this unaccounted-for strength of slabs due to boundary conditions can only be utilized if the designer knows the degree of restraints present.

Since the theoretical model was verified only on small scale models, it was decided to test a number of existing decks in order to determine its applicability for prototypes. Existing decks, generally deteriorated to varying degrees, with variable supporting elements were subsequently load tested.

Objectives

The three main objectives of the field testing of existing decks were as follows:

1. To ensure that no slab failure is caused by a concentrated test load of 445 kN (100 kips). This no-failure criterion for existing deteriorated decks ensures a factor of safety of 5 against the maximum measured wheel loads of 90 kN (20 kips) in Ontario.

2. To determine if different types of slab and girder bridges provide different degrees of confinement or restraint. For example, is there a difference in slab strength, due to restraint factor, between composite and non-composite slabs, or between concrete and steel girders? Consequently, the test bridges chosen were of four categories:

Type	
A	Non-composite steel girder and concrete slab.
B	Composite steel girder and concrete slab.
C	Concrete beam and slab (monolithic).
D	Composite AASHTO girders and concrete slab.

3. To establish the lower bound restraint factors for each category. These factors were to be based on a comparison between the experimental data and the theoretical analysis.

Testing Procedure

Prior to the testing program, a total of 40 bridges were chosen to obtain a wide range of parameters of span, slab thickness, age, deterioration, bridge type and reinforcing. Due to testing difficulties and/or lack of sufficient data regarding the concrete deck and its strength, data from only 32 bridges were examined and included. There were 13 Type A, 9 Type B, 8 Type C, and 2 Type D bridges. These were generally older structures and had deteriorated to varying degrees of disrepair by the time of testing.

The testing apparatus is shown in Figure 3. The test load of 445 kN (100 kips) is hydraulically controlled and applied through the loading apparatus attached to the underside of the trailer. The test vehicle has a weight of 212 kN (47.8 kips) and is loaded with 378 kN (85.0 kips) of concrete blocks for a total load of 490 kN (132.8 kips). The test load is applied, by a hydraulic ram, through two 254 mm (10 in.) square pads with a 76 mm (3 in.) space between them. These loading pads simulate the footprint of a dual tire wheel.

Once the load positions were established, the load was gradually applied and the deflection at the point of load application, as well as the load recorded on an X-Y plotter. The load was monitored by a pressure transducer and the displacement measured by a transducer riding on a 3.7 m (12 ft.) long aluminum bar simply supported at the ends as shown in Figure 3. Accordingly, the measured displacement is based on the assumption that the support points of the bar, being remote from the load position, exhibit insignificant vertical movements. The orientation of the bar was always parallel to the traffic lanes.

Test Results

Figure 4 illustrates a typical test plot of load versus deflection. As can be seen, the test consists of applying the test load in a cyclic manner until the load-vs-deflection plot is repetitive and shows no further progressive permanent deflection upon application of load.

With each test bridge, an attempt was made to obtain concrete cores near the test points. Thereby, the effect of matured strength of the concrete deck due to time could be included in the evaluation of the results. The compressive strength of the various decks varied from 18.6 MPa (2,700 psi) to 75.8 MPa (11,000 psi).

The first objective of ensuring no-failure for loads of 445 kN (100 kips) was accomplished since no failures of any continuous decks were observed. Two failures have occurred, on the same bridge, at loads of 288 kN (65 kips) and 360 kN (81 kips), respectively. In both cases, the concrete was so deteriorated that cores could not be taken and the slab, being at the edge of a cantilever, had no lateral restraint whatsoever.

This ultimate strength theory predicts that, with typical reinforcement level of 0.8% and with zero restraint, the deck failure load is between 445 and 670 kN (100 and 150 kips). For a 20.7 MPa (3,000 psi) concrete and a load of 445 kN (100 kips), the vertical shear stress, computed on the perimeter of the critical section at d/2 from load is 1.45 MPa (210 psi) or $4\sqrt{f'c}$. In other words, vertical shear failure could not be expected even if present code requirements were applied.

No serious structural cracking was noticed in any of the slabs. No visible cracking on the top surface of the slab in the transverse negative moment regions above the longitudinal girders was ever noticed. Directly under the load on the bottom surface of the deck, hairline cracking was observed during the tests, however, the cracks disappeared upon removal of the load.

The presence of boundary restraint was expected to significantly increase the punching shear capacity of bridge decks. Boundary restraint is provided by prohibiting the free movement of the slab, in both rotation and lateral movement. This restraint is provided by the main beams, the lateral bracing and the slab itself. The boundary restraint is difficult to calculate and the difficulty is further complicated by the large variety of bridges that exist and that can be designed. With this situation, the bridges tested were subdivided into the four categories as defined above, to see if a significant difference in boundary restraint exists among them. The value of restraint factor, F_r, is based on the Queen's study by B.deV. Batchelor and B.E. Hewitt (5) and is empirically taken between zero for no restraint and 1.0 for absolute restraint.

The comparison between experimental and theoretical results is based on measured and theoretical deflections. During the testing, plots of load versus deflection (as illustrated in Figure 4) were obtained. These were then compared with theoretical deflections for restraint factors of 0.25, 0.50, 0.75 and 1.00, in order to establish the actual restraint factor for each bridge. The deflection and ultimate load-carrying capacity were provided by the computer program developed at Queen's University (5). These ultimate deflections were then linearly interpreted to correspond to the 445 kN (100 kips) test load in order to estimate the actual restraint factor present. The following factors were considered; slab thickness and span, reinforcement ratio, effective slab thickness, slab span, applied load area and concrete strength. Experimental deflections and deck parameters are provided in Tables 1 to 4.

Table 5 shows the predicted restraint factors present and only tests where actual concrete strengths were available are included. The data indicate the presence of boundary restraint for all four classifications. The non-composite girder/concrete slab bridges exhibit the smallest average F_r of 0.41. A safe lower bound value would appear to be 0.20. The other three types, which are all of composite construction, exhibit average F_r values between 0.78 and 0.93, with a lower bound value of 0.40. There appears to be no significant difference between Types B, C and D. Maximum variation in restraint factor is in Type C while Type B has the highest overall restraint factor.

For the test results, the deflection/span ratios varied between 1/100 to 1/900 for the non-composite and between 1/900 to 1/3500 for composite slabs. Although a large variation is present, the non-composite slabs generally exhibit deflections three times larger than the corresponding composite slabs. This suggests that the composite slab exhibits a greater restraint factor since there is a positive connection to the main load-carrying members.

It should be noted that the above results are based on small deflection results [a maximum of 8.6 mm (0.34 in.)]; consequently, small experimental errors could potentially result in a large percentile error. Experimental errors may have occurred from the following sources: movement of reference points, instability of asphalt wearing surface, calibration of testing equipment, and friction in the hydraulic ram. These factors, and the large variation in the restraint factors obtained from this testing program, therefore, lead to general rather than detailed recommendations.

References 6 and 7 describe extensive prototype testing on bridge decks designed to the provisions of the new theory employing a reduced steel ratio of 0.3%. Although the tests were rather encompassing, no bottom steel exhibited stress in excess of 230 MPa (33 ksi) for bottom reinforcement under the 445 kN (100 kips) test load. This corresponds to a stress level of 46 MPa (6.7 ksi) for the observed maximum half axle weight of 90 kN (20 kips). No stress in excess of 35 MPa (5.0 ksi) was ever measured on negative reinforcement indicating the inadequacy of the AASHTO strip equation.

Appendix A is devoted to a parametric study regarding a simply-supported beam exposed to a single concentrated load with varying lateral displacement and rotational restraints. While it is understood that three-dimensional behavior can differ from this quantitatively, the authors believe that the analogy presented will provide some insight to the subject matter.

Summary and Conclusions

The punching shear testing of existing thin concrete decks indicates that there is a very large capacity against failure that can now be identified. The research at Queen's (4, 5) shows that for typical decks, a punching failure of the slab should occur prior to any flexural failure. The test load of 445 kN (100 kips), representing a dual-tired wheel, is 10 times larger than the allowable legal load and 4 to 5 times larger than the maximum half-axle weight observed. Even under this heavy overload, combined with the deterioration of some decks, no failures of restrained decks were ever observed. Consequently, these slabs can be considered to be greatly overdesigned as they showed no sign of structural damage due to simulated wheel loads.

As a general conclusion for the concrete decks tested, a restraint factor of 0.25 may be assumed for non-composite decks; for composite decks, a factor of 0.50 may be assumed. These lower bound tentative values may be safely used to design more economic slabs. The aspect of crack control must still be investigated however large cracking can be eliminated by providing small bar sizes at close spacing.

For a typical concrete deck, based on the AASHTO working stress design, the theoretical ultimate strengths are presented in Table 6.

Theoretical ultimate strengths for a concrete deck with 0.2% reinforcing steel ratio, which is typically the minimum steel ratio for temperature and shrinkage requirements, are also shown. It can be seen that a typical slab having an AASHTO design load of 93.6 kN (20.8 kips) live load plus impact with a restraint factor of 0.5 has a factor of safety against failure of 14.5. Furthermore, the 80% reduction in steel results in only a 28% reduction in ultimate capacity.

Table 7 shows the factor of safety for the above decks for various restraint factors. Assuming a lower bound restraint factor of 0.5 for composite decks, the minimum factor of safety based on a wheel load of 93.6 kN (20.8 kips) is 10.4.

Substantial savings in construction costs can be obtained by revising the design of concrete decks of this type. The design should be based on the actual collapse mechanism of the decks and not on an elastic approach as outlined in the AASHTO Specifications. The savings, resulting from reducing the reinforcing steel by 80%, are approximately $\$15/m^2$ ($1.40/sq. ft.), or approximately $10,000 for a 2-lane, 61 m (200 ft.) span bridge. Further cost benefits of reduced construction time, reduced maintenance and standardization of reinforcement will also be realized.

Recommendations

It is strongly suggested that the design approach as specified by AASHTO should be discontinued for decks within the parameters outlined. The deck strength developed by restraining boundary conditions should be utilized by basing the design on the theory developed at Queen's University (4,5).

It is recommended that thin concrete decks of composite construction and within the outlined design parameters be designed by assuming a restraint factor (F_r) of 0.5. Consequently, an isotropic reinforcing steel ratio of 0.2 is sufficient for standard decks. For better crack control for live loads, shrinkage and temperature, however, a ratio of 0.3% should be used.

Figure 5 shows a welded wire mesh recommended for use in a standard 200 mm (8 in.) 2-stage construction deck. This is a suggested method of standardization for new concrete thin deck construction. The 150 mm (6 in.) base concrete will have reinforcement as shown. The 50 mm (2 in.) high quality concrete will provide a skid resistant riding surface and ensure proper cover and protection against the rusting of the reinforcing steel. The reinforcement consisting of welded wire mesh with integral supports will provide a sufficiently rigid reinforcing mat. The welded wire mesh of gauge 5/0½ steel at 200 mm (8 in.) centers, for both top and bottom layer would be prefabricated and uniform throughout the entire length of the deck and simply placed on the framework. This welded wire mesh provides a reinforcing steel area of 13 mm^2 (0.2 sq. in.). This type of reinforcement spaced in 200 mm (8 in.) modules could become standard in bridge deck design and construction.

As the AASHTO-recommended large negative moments do not seem to materialize on the bridges tested, it appears that a cover of 76 mm (3 in.) in a 200 mm (8 in.) deck can be safely permitted. For #4 bars, this would give a cover/diameter ratio of 6 which is considered absolute protection against the ingress of salt. The future might see bridge decks built in a single course, with 0.2% reinforcement under 76 mm (3 in.) cover requiring no additional protection.

References

1. Standard Specifications for Highway Bridges. American Association of State Highway and Transportation Officials, 1973.
2. Interim Specifications, Bridges 1974. American Association of State Highway and Transportation Officials, 1974.
3. D.C. Manning and J. Ryell. Durable Bridge Decks. RR203, Ontario Ministry of Transportation and Communications, Downsview, Ontario, Canada, 1976.
4. B. deV. Batchelor, B.E. Hewitt, P.F. Csagoly and M. Holowka. An Investigation of the Ultimate Strength of Deck Slabs of Composite Steel/Concrete Bridges. Proceedings of the Bridge Engineering Conference, TRB, St. Louis, Missouri, 1978.
5. B.E. Hewitt and B. deV. Batchelor. Punching Shear Strength of Restrained Slabs. Journal of the Structural Division, ASCE, Vol. 101, No. St9, September 1975, pp. 1837-1853.
6. R.A. Dorton, M. Holowka and J.P.C. King. The Conestogo River Bridge — Design and Testing. Canadian Journal of Civil Engineering, Vol. 4, No. 1, 1977, pp. 18-39.

Table 1. Steel beam and concrete slab (non-composite).

Bridge Number	Stringer Spacing (m)	Stiffener Spacing (m)	Slab Thickness (mm)	Main Rebars (mm)	Distribution Rebars (mm)	Experimental Deflection (mm)	Concrete Strength (MPa)	Restraint Factor (F_r)
S1	1.83	3.81	180	#5 @ 305 (T) #5 @ 150 (B)	#5 @ 305 (T) #5 @ 150 (B)	3.56 3.81	52.5 62.7	0.25 0.23
S2	1.74	4.78	180	#5 @ 150 (T) #5 @ 150 (B)	#5 @ 455 (T) #5 @ 915 (B)	2.29 5.08 4.57	54.7 54.7 40.8	0.33 0.20 0.21
S14	1.75	7.62 to 4.72	180	#5 @ 150 (T + B)	#5 @ 455 (T + B)	2.29 2.79	53.7 43.5	0.33 0.31
S17	2.84	9.14	215	#5 @ 125 (T + B)	#4 @ 510 (T + B)	1.52	41.5	0.71
S32	3.45	3.56	180	#5 @ 150 (T + B)	#5 @ 150 (T + B)	5.08 4.82	32.5 36.4	0.63 0.61
S34	1.83	6.10 to 7.01	180	#5 @ 150 (T + B)	#4 @ 380 (B)	3.56	52.5	0.24
S35	1.52 to 1.84	6.10 to 7.21	180	#5 @ 150 (T + B)	#5 @ 535 (T) #5 @ 455 (B)	2.79 1.78	26.8 44.3	0.34 0.55
S37	3.51	3.12	215	#6 @ 150 (T + B)	#6 @ 150 (T + B)	3.30	19.3	1.00
S39	1.52	3.05	180	#5 @ 150 (T + B)	#4 @ 380 (T + B)	3.56 2.54	27.49 38.52	0.21 0.25

1 ft. = 0.3048 m 1 in. = 25.4 mm 1 psi = 6.89 x 10^3 MPa 1 psi = 6.89 kPa

Table 2. Steel beam and concrete slab (composite).

Bridge Number	Stringer Spacing (m)	Stiffener Spacing (m)	Slab Thickness (mm)	Main Rebars (mm)	Distribution Rebars (mm)	Experimental Deflection (mm)	Concrete Strength (MPa)	Restraint Factor (F_r)
S23	2.74	5.79 to 8.23	205	#6 @ 230 (T + B)	#4 @ 380 (T) #4 @ 430 (B)	0.71 0.84 1.17	27.6 (design)	1.0 1.0 1.0
S38	2.13	5.49	205	#6 @ 250 (T + B)	#4 @ 305 (T + B)	1.60 1.50 1.02	29.6 27.6 (est) 27.6 (est)	0.75 0.83 1.00
S18	1.93	5.72	180	#5 @ 150 (T + B)	#5 @ 305 (T + B)	1.78	18.9	1.00
S37	3.51	3.15	215	#6 @ 150 (T + B)	#6 @ 150 (T + B)	3.05 2.80	48.6 27.6 (est)	0.80 1.00
B1	1.93	4.46	195	#5 @ 150 (T + B)	#5 @ 380 (T + B)	1.65	27.6	0.96
B2	2.59	7.51	195	#5 @ 150 (T + B)	#5 @ 305 (T + B)	1.78	37.3	0.75
B3	1.83	4.34	190	#6 @ 230 (T + B)	#4 @ 230 (T + B)	1.35	28.5	1.00
B4	1.83	4.57	180	#6 @ 230 (T + B)	#4 @ 230 (T + B)	1.65	25.1	0.98
B5	3.17	6.74	215	#5 @ 150 (T + B)	#5 @ 305 (T + B)	1.78	38.00	0.94

1 ft. = 0.3048 m 1 in. = 25.4 mm 1 psi = 6.89 x 10^3 MPa 1 psi = 6.89 kPa

Table 3. Concrete beam and concrete slab (monolithic).

Bridge Number	Stringer Spacing (m)	Stiffener Spacing (m)	Slab Thickness (mm)	Main Rebars (mm)	Distribution Rebars (mm)	Experimental Deflection (mm)	Concrete Strength (MPa)	Restraint Factor (F_r)
S3	3.15	7.01 & 10.36	200	#5 @ 150 (T + B)	unknown	1.40	42.9	1.0
S5	7.77	2.13	215	#5 @ 280 (T) #5 @ 140 (B)	#4 @ 535	0.58 0.97 0.99 0.71	67.9 60.1 66.0 60.1	0.75 0.50 0.48 0.71
S6	3.20	10.36	255	#5 @ 190 (T + B)	#4 @ 305	0.46 0.48 0.37	76.1 74.2 56.6	0.75 0.75 0.75
S10	2.95	3.74	230	#5 @ 150 (T + B)	#5 @ 455 (T + B)	0.71 0.71 0.38	61.1 71.1 55.9	0.75 0.63 1.00
S15	3.04	5.49 & 7.32	180	#4 @ 125 (T + B)	#4 @ 610 (T + B)	1.27	42.6	1.00
S22	1.83	4.80	200	#4 @ 150 (T + B)	#4 @ 455 (T + B)	1.52	68.3	0.40
S32	3.30	–	200	#5 @ 150 (T + B)	#4 @ 610 (T) #4 @ 510 (B)	2.29 1.45	36.4	0.82 1.00
S42	1.93	–	200	#5 @ 280 (T) #5 @ 140 (B)	#4 @ 510 (B)	0.28 0.25 0.28	27.6 (assumed)	1.00 (all)

1 ft. = 0.3048 m 1 in. = 25.4 mm 1 psi = 6.89 x 10^3 MPa 1 psi = 6.89 kPa

Table 4. AASHTO girders and concrete slab (composite)

Bridge Number	Stringer Spacing (m)	Stiffener Spacing (m)	Slab Thickness (mm)	Main Rebars (mm)	Distribution Rebars (mm)	Experimental Deflection (mm)	Concrete Strength (MPa)	Restraint Factor (F_r)
S16	2.51	6.10	190	#5 @ 125 (T + B)	#5 @ 300 (T) #5 @ 200 (B)	1.78	64.9	0.66
S33	2.21	14.63	190	#6 @ 165 (T + B)	#5 @ 455 (T) #5 @ 180 (B)	1.27	32.5	1.00

1 ft. = 0.3048 m 1 in. = 25.4 mm 1 psi = 6.89×10^3 MPa 1 psi = 6.89 kPa

Table 5. Predicted effective restraints in bridges tested.

Type A: Non-Composite Steel Girder and Concrete Slab		Type B: Composite Steel Girder and Concrete Slab		Type C: Concrete Beam and Slab - Composite		Type D: AASHTO Girder and Concrete Slab - Composite	
Bridge Number	F_r	Bridge Number	F_r	Bridge Number	F_r	Bridge Number	F_r
S1	0.23, 0.25	S18	1.0	S3	1.0	S16	0.66
S2	0.21, 0.33	S23	1.0, 1.0, 1.0	S5	0.48, 0.50	S33	1.0
S14	0.31, 0.33	S37	0.8, 1.0		0.71, 0.75		
S17	0.71	S38	0.75, 0.83, 1.0	S10	0.63, 0.75, 1.0		
S32	0.61, 0.63	B1	0.96	S15	1.0		
S34	0.24	B2	0.75	S22	0.40		
S35	0.34, 0.55	B3	1.0	S32	0.82, 1.0		
S37	1.0	B4	0.98	S42	1.0, 1.0		
S39	0.21, 0.25	B5	0.94	S6	0.75, 0.75, 0.75		
Average Restraint	0.41	Average Restraint	0.93	Average Restraint	0.78	Average Restraint	0.83

Table 6. Ultimate strength of decks.

	Theoretical Ultimate Strength	
Restraint Factor	Reinforcing Steel Ratio = 0.01	Reinforcing Steel Ratio = 0.002
0.0	810 kN (183 kips)	210 kN (47 kips)
0.25	1080 kN (243 kips)	610 kN (137 kips)
0.50	1340 kN (302 kips)	960 kN (216 kips)

Deck Description:

Span = 2.44 m (8 ft.)
Thickness = 200 mm (8 in.)
Effective depth = 165 mm (6.5 in.)
Concrete strength = 27.6 MPa (4000 psi)
Reinforcing steel ratio = 0.009 to 0.002
Yield strength = 413 MPa (60,000 psi)

Table 7. Factor of safety of decks.

Typical Structure with Various Restraint Factors	1% Reinforcement		0.2% Reinforcement	
	f'_c = 27.6 MPa	f'_c = 34.5 MPa	f'_c = 27.6 MPa	f'_c = 34.5 MPa
0.0	8.8	9.2	2.3	2.3
0.25	11.7	12.9	6.6	7.7
0.50	14.5	16.5	10.4	12.4
0.75	17.5	20.3	13.9	16.7
1.00	20.6	24.2	17.1	20.6

1 MPa = 145 psi

Figure 1. Concrete slab load capacity.

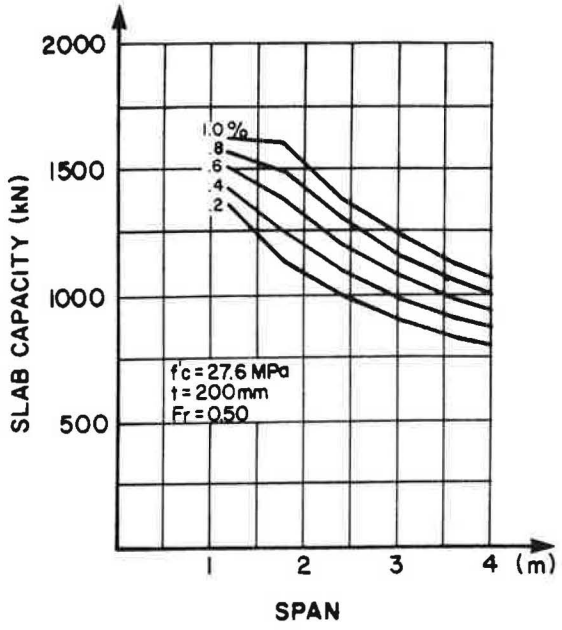

Figure 2. Arching action in deck slabs.

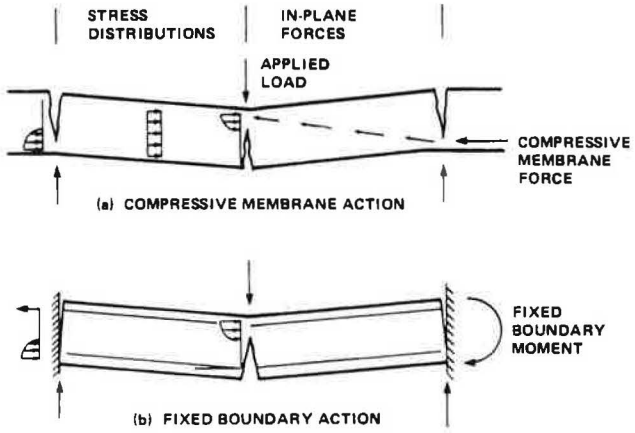

Figure 3. Overall view of typical testing apparatus.

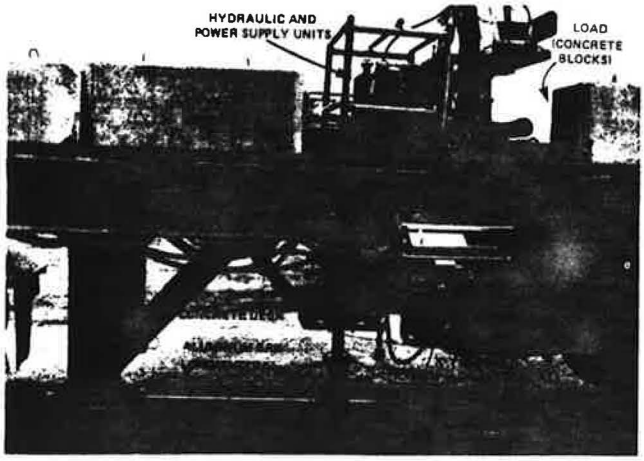

Figure 4. Plot of typical load vs. deflection curve.

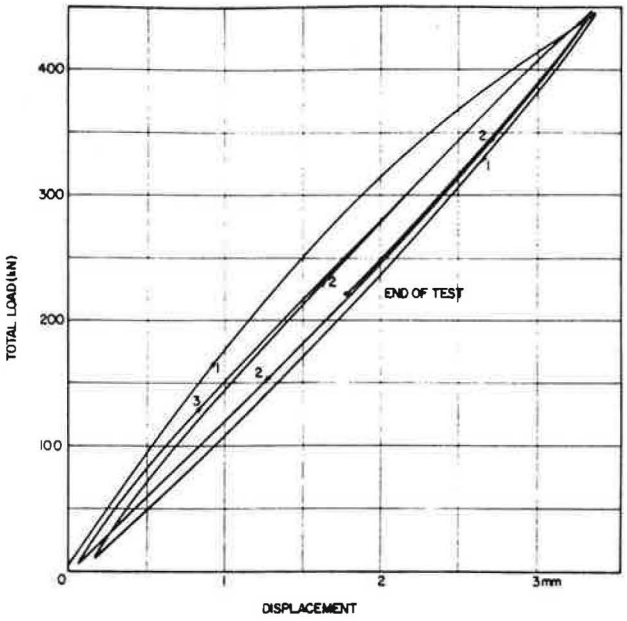

Figure 5. Standard prefabricated steel reinforcement.

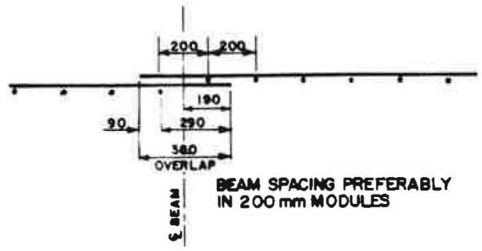

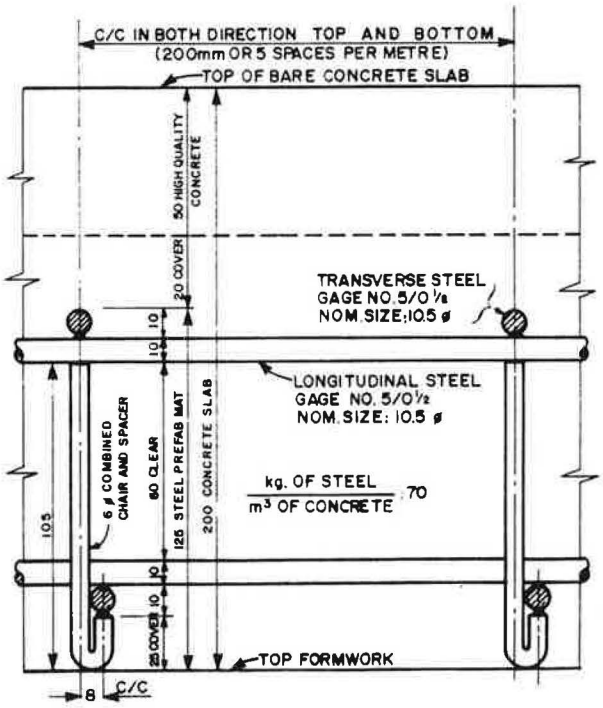

Appendix A, Effect of Boundary Restraints

The effect of boundary restraints and the resulting boundary forces can be qualitatively illustrated by the simple beam model shown in Figure A.1. The beam is loaded by a central point load (P) and the ends are restrained against free movement by a horizontal force (H) and a moment (M) which act at a distance (a) from the bottom surface of the beam. In a reinforced concrete beam, these forces would be assumed to act at the reinforcing steel level. Figure A.1 also shows the moment diagram for all three forces.

Since M and H are the unknown variables, the following equations can be used to solve for M and H in terms of P by equating displacements:

$$\Delta_{HH}\, H + \Delta_{HM}\, M = \Delta_{HP} \qquad (1)$$

$$\Delta_{MH}\, H + \Delta_{MM}\, M = \Delta_{MP} \qquad (2)$$

The magnitude of the horizontal force and moment depends on the rotational and lateral resistance of the boundary. Two additional variables can be defined as:

- F = lateral resistance, defined as the force required to move the boundary by unit length, and
- K = flexural resistance, defined as the moment required to move the boundary by unit rotation.

After resolving equations 1 and 2, and substituting the appropriate parameters, the following expressions are obtained:

$$M = \frac{1.5\, P\ell^2\, Kh^2\, F\ell + 2Eh}{h^2\, [\ell\rho F + 2Eh]\, [12\ell K + 2Eh] - 144e^2\ell^2 FK} \qquad (3)$$

and

$$H = \frac{3P\ell^2\, eEFh^3}{h^2\, [\ell\rho F + 2Eh]\, [12\ell K + 2Eh^3] - 144e^2\ell^2 FK} \qquad (4)$$

where h = overall height
e = 0.5h - a
a = distance from bottom surface to location of force (H)
α = e ÷ h
ρ = 1 + 12α^2
I = $h^3/12$ (assuming a unit width)
A = h (assuming a unit width)
E = modulus of elasticity

If the value of K is taken as a function of the adjacent span then,

$$K = \frac{3EI}{\bar{\ell}} = \frac{Eh^3}{4\bar{\ell}}$$

where $\bar{\ell}$ = the length of adjacent span

If the value of F is taken as a function of the surrounding slab then,

$$F = \frac{EA}{\ell} = \frac{EhN}{\ell}$$

where N = the number of strips of unit width providing lateral confinement for the strip under consideration.

By substituting the above relationships into equations 3 and 4, the following expressions for M and H are obtained:

$$M = \frac{3P\ell}{8}\gamma \qquad (5)$$

where

$$\gamma = \frac{j\,(N+2)}{[\rho N + 2]\,[3_j + 2] - 36\alpha^2 N_j} \qquad (5a)$$

j = the ratio of length of the span under consideration and the adjacent span length.

and

$$H = \frac{3P\ell}{h}\beta \qquad (6)$$

where

$$\beta = \frac{\alpha N}{[\rho N + 2]\,[3_j + 2] - 36\alpha^2 N_j} \qquad (6a)$$

By using Figure A.1, top and bottom surface stresses can be obtained for this beam:

$$f_r = \frac{P\ell}{4}\cdot\frac{6}{h^2} + \frac{3P\ell}{h}\,\beta\cdot\frac{1}{h} - \frac{3P\ell}{h}\,\beta\cdot e\cdot\frac{6}{h^2} - \frac{3P\ell}{8}\cdot\gamma\cdot\frac{6}{h^2}$$

$$f_T = \frac{3P\ell}{h^2}\left[+\frac{1}{2} + \beta - 6\beta\alpha - \frac{3\gamma}{4}\right] \qquad (7)$$

and

$$f_B = \frac{3P\ell}{h^2}\left[-\frac{1}{2} + \beta + 6\beta\alpha + \frac{3\gamma}{4}\right] \qquad (8)$$

It can be seen from equations 7 and 8 that the expression in brackets is a variable depending on the degree of restraint. With M and F equal to zero, equations 7 and 8 give the stress expected for a simply-supported beam.

Where

$$f_T = f_B = \frac{P\ell}{4}\,\frac{6}{h^2} = \frac{1.5\,P\ell}{h^2}$$

equations 7 and 8 indicate that the stress, with or without restraint, increases with the span length and decreases with the square of the beam thickness.

By assuming typical concrete deck slab dimensions, the effect of varying lateral and flexural restraint can be illustrated. For a typical 200 mm (8 in.) beam, e_{min} can be estimated to be 65 mm (2.5 in.). The span length ratio (j) is varied between 0.50 and 2.00, while the ratio (N) is varied between 1 and infinity. Figure A.2 illustrates the effect of the varying restraint.

For the top stresses (Figure A.2a), increasing adjacent slab spans decrease the stress coefficients while the horizontal restraint, irrespective of its effective width, has a very small effect on the top stresses.

Figure A.2b indicates that both lateral and horizontal restraint has an effect on the bottom surface stresses. The stress coefficient decreases with increasing slab span ratio and increasing effective width of lateral restraint width.

Figure A.3 shows the effect on the bottom stress coefficient of a varying lateral restraint with zero rotational restraint. The stress coefficient varies inversely with N and with full restraint, the case where N is infinite, the

limiting value of the stress coefficient is 0.2923. As previously mentioned, this stress coefficient is equal to 0.50 with zero lateral and rotational restraint. For this case, the effect of different e values (where e is the eccentricity between the location of the restraining force and the neutral axis) was also investigated. The above stress coefficient decreases with increasing e as expected. For a 25 mm (1 in.) increase in e, the stress coefficient decreases by 12%.

The parametric study of a simply-supported beam loaded by a single concentrated load with varying lateral displacement and rotational restraints indicates that the extreme fiber stresses are significantly lower (by up to 45%) than extreme fiber stresses with zero restraint.

Figure A.1. Simply-supported beam of rectangular cross section.

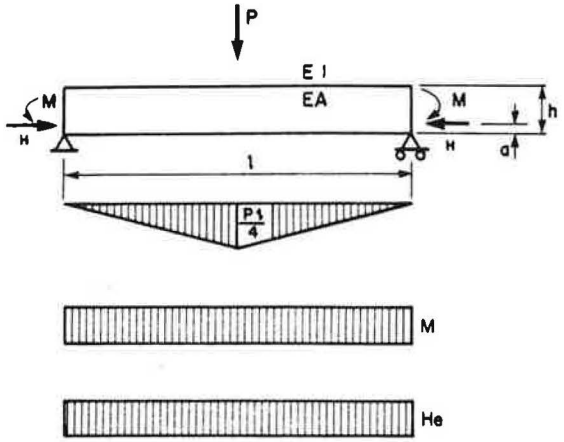

Figure A.2(a). Effect of varying restraint values (top face of slab).

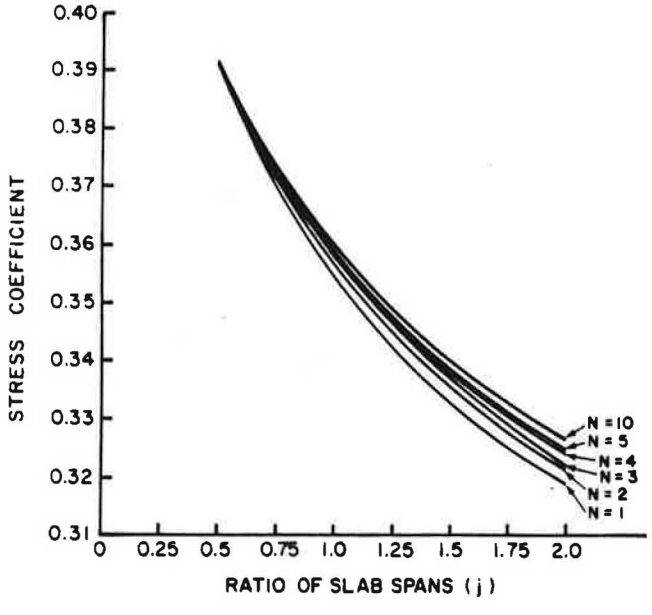

(a) TOP FACE OF SLAB

Figure A.2(b). Effect of varying restraint values (bottom face of slab).

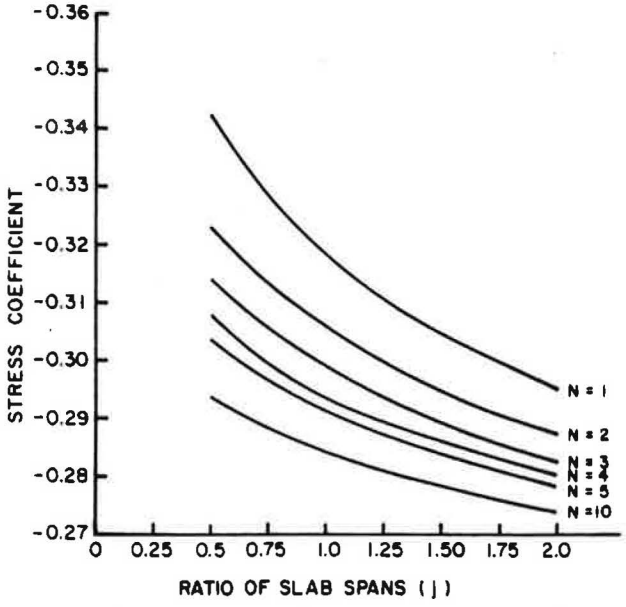

(b) BOTTOM FACE OF SLAB

Figure A.3. Variation of stress coefficient with lateral restraint (assuming zero rotational restraint).